Interdicting G_q Activation in Airway Disease by Receptor-Dependent and Receptor-Independent Mechanisms

Richard Carr III, Cynthia Koziol-White, Jie Zhang, Hong Lam, Steven S. An, Gregory G. Tall, Reynold A. Panettieri, Jr., and Jeffrey L. Benovic

Department of Biochemistry and Molecular Biology, Thomas Jefferson University, Philadelphia, Pennsylvania (R.C., J.L.B.); Department of Medicine, Pulmonary, Allergy, and Critical Care Division, Airways Biology Initiative, University of Pennsylvania Perelman School of Medicine, Philadelphia, Pennsylvania (C.K.W., J.Z., R.A.P.); Department of Environmental Health Sciences, Johns Hopkins Bloomberg School of Public Health, Baltimore, Maryland (H.L., S.S.A.); and Department of Pharmacology and Physiology, University of Rochester Medical Center, Rochester, New York (G.G.T.)

ABSTRACT

$G\alpha_q\beta\gamma$ heterotrimer (G_q), an important mediator in the pathology of airway disease, plays a central role in bronchoconstriction and airway remodeling, including airway smooth muscle growth and inflammation. Current therapeutic strategies to treat airway disease include the use of muscarinic and leukotriene receptor antagonists; however, these pharmaceuticals demonstrate a limited clinical efficacy as multiple G_q-coupled receptor subtypes contribute to these pathologies. Thus, broadly inhibiting the activation of G_q may be an advantageous therapeutic approach. Here, we investigated the effects of broadly inhibiting G_q activation in vitro and ex vivo using receptor-dependent and receptor-independent strategies. P4pal-10 is a protease activated receptor 4–derived pepducin that exhibits efficacy toward multiple G_q-coupled receptors. Mechanistic studies demonstrated that P4pal-10 selectively inhibits all G protein coupling to several G_q-coupled receptors, including protease activated receptor 1, muscarinic acetylcholine M3, and histamine H1 receptors, while demonstrating no direct effect on G_q. We also evaluated the ability of FR900359, also known as UBO-QIC, to directly inhibit G_q activation. FR900359 inhibited spontaneous $G\alpha_q$ nucleotide exchange, while having little effect on $G\alpha_s\beta\gamma$, $G\alpha_i\beta\gamma$, or $G\alpha_{12/13}\beta\gamma$ heterotrimer activity. Both P4pal-10 and FR900359 inhibited G_q-mediated intracellular signaling and primary human airway smooth muscle growth, whereas only FR900359 effectively interdicted agonist-promoted airway contraction in human precision cut lung slices. These studies serve as a proof of concept that the broad-based inhibition of G_q activation may be a useful therapeutic approach to treat multiple common pathologies of airway disease.

Introduction

Asthma manifests as a complex respiratory syndrome of airway hyperresponsiveness and inflammation. Airway smooth muscle (ASM) shortening evokes an airway obstruction that clinically manifests as a significant decrease in peak airflow (Deshpande and Penn, 2006). Common therapeutic interventions include the use of glucocorticoids to curb airway inflammation and are often combined with a long-acting β-agonist. Other therapies include leukotriene and muscarinic receptor antagonists that inhibit the activation of $G\alpha_q\beta\gamma$ heterotrimer (G_q)-coupled receptors that mediate the parasympathetic and hormonal signaling regulating bronchomotor tone (Bel, 2013). G protein–coupled receptor (GPCR) antagonists have a somewhat limited efficacy in patients as the activation of multiple G_q-coupled receptors contribute to the pathology of the disease (Scadding and Scadding, 2010; Moulton and Fryer, 2011). It is plausible that inhibiting G_q activation at the receptor or G protein level would be an advantageous asthma therapeutic as G_q-mediated ASM shortening is a primary contributor to bronchotone (Borchers et al., 2003; Pelaia et al., 2008).

P4pal-10 is a pepducin antagonist derived from intracellular loop 3 of protease-activated receptor (PAR) 4 (Covic et al., 2002). In the initial report, P4pal-10 demonstrated efficacy in preventing PAR4-mediated platelet activation ex vivo and exhibited antithrombotic activities in vivo. Interestingly, P4pal-10 inhibited both PAR1- and PAR4-mediated platelet aggregation and it was suggested this was due to disruption of

ABBREVIATIONS: AP, agonist peptide; β_2AR, β_2-adrenergic receptor; ASM, airway smooth muscle; BSA, bovine serum albumin; CXCR, CXC chemokine receptor; DMSO, dimethylsulfoxide; DPBS, Dulbecco's phosphate-buffered saline; DTT, dithiothreitol; EGF, epidermal growth factor; Fura2-AM, Fura-2 acetoxymethyl ester; $G_{12/13}$, $G\alpha_{12/13}\beta\gamma$ heterotrimer; G_i, $G\alpha_i\beta\gamma$ heterotrimer; G_q, $G\alpha_q\beta\gamma$ heterotrimer; G_s, $G\alpha_s\beta\gamma$ heterotrimer; GPCR, G protein–coupled receptor; GST, glutathione S-transferase; GTPγS, guanosine 5'-O-[gamma-thio]triphosphate; HBSS, Hank's balanced salt solution; HEK, human embryonic kidney; PAGE, polyacrylamide gel electrophoresis; PAR, protease activated receptor; P4pal-10 Scr, scrambled P4pal-10; RBD, Rhotekin Rho-binding domain; SDS, sodium dodecyl sulfate; TBST, Tris-buffered saline with Tween 20; TXA2R, thromboxane A2 receptor.

the activity of PAR1/PAR4 heterodimers and loss of responsiveness from both receptor subtypes. Moreover, although Covic et al. reported that P4pal-10 had little effect on thromboxane A2 receptor (TXA$_2$R) function in platelets (Covic et al., 2002), other investigators reported that TXA$_2$R was sensitive to P4pal-10 in human platelet aggregation at concentrations comparable to those used to inhibit PAR1 and PAR4 (Stampfuss et al., 2003). Here, we further investigated the putative multiple efficacies of P4pal-10 and applied its unique properties to understand the mechanisms and application of broad-based G$_q$ inhibition in the treatment of airway disease.

The relative therapeutic advantage of broad-based G$_q$ inhibition was also studied using a small molecule inhibitor of G$_q$ activation, FR900359 (also known as UBO-QIC). FR900359 is a cyclic depsipeptide isolated from the roots of *Ardisia crenatasims* that is nearly structurally identical to the well studied G$_q$ inhibitor YM-254890 (Fujioka et al., 1988; Taniguchi et al., 2003; Takasaki et al., 2004; Bernard et al., 2014). Although not as well characterized as YM-254890, FR900359 likely retains the same properties and mode of operation. Structural studies of a YM-254890/Gα_q complex revealed that the compound interacts with the hinge region between the α-helical domain and GTPase domain of Gα_q (Nishimura et al., 2010). These contacts may inhibit the opening of the nucleotide-binding pocket that is requisite for GDP/GTP exchange and subsequent G protein activation. Recent studies using FR900359 demonstrate efficacy in inhibiting G$_q$-mediated signaling in human platelets, with little effect on the activity of G$\alpha_s\beta\gamma$ heterotrimer (G$_s$), G$\alpha_i\beta\gamma$ heterotrimer (G$_i$), or G$\alpha_{12/13}\beta\gamma$ heterotrimer (G$_{12/13}$) (Inamdar et al., 2015). Further, the proposed vasorelaxant properties were confirmed in an ex vivo model of rat aortic relaxation (Zaima et al., 2013). FR900359 has also been used as a molecular tool to dissect cellular signaling pathways that include the influence of Gβ5-RGS7 complex formation on G$_q$-mediated calcium flux (Karpinsky-Semper et al., 2014). Here, we assessed the ability of FR900359 to inhibit G$_q$-dependent airway smooth muscle growth and airway contraction.

Materials and Methods

Materials. P4pal-10 (palmitate-SGRRYGHALR-amide), scrambled P4pal-10 (P4pal-10 Scr) (almitate-YLHARGSRGR-amide), and PAR1–agonist peptide (AP) (SFLLRN) were synthesized by an Fmoc solid-phase protocol and purified to >98% by C18 reverse-phase chromatography (Peptide2.0). FR900359 was acquired under the name of UBO-QIC from the Pharmazeutische Biologie at the Universität Bonn (Bonn, Germany). Pertussis toxin from *Bordetella pertussis*, adenosine 5′-triphosphate disodium salt hydrate (99%), bradykinin (RPPGFSPFR) acetate salt (99%), forskolin from *Coleus forskohlii* (≥98%), (−)-isoproterenol hydrochloride (≥98%), and histamine (≥97%) were purchased from Sigma-Aldrich (St. Louis, MO). Carbamylcholine chloride (carbachol, 99%) was purchased from Acros Organics (Fischer Scientific, Geel, Belgium). Purified recombinant human Stromal-derived factor 1α was obtained from ProSpec (East Brunswick, NJ).

Cell Culture. Human embryonic kidney (HEK) 293 and HeLa cells were cultured in Dulbecco's modified Eagle medium (CellGro, Tewksbury, MA) supplemented with 10% fetal bovine serum. Primary human airway smooth muscle cells were isolated from donors, with no known chronic illness or medication use, as previously described (Panettieri et al., 1989). Passages 4–7 ASM cells were maintained in complete medium (Ham's F-12 medium supplemented with 10% fetal

bovine serum, 25 mM HEPES, pH 7.2, 1.7 mM CaCl$_2$, 2 mM L-glutamine, 0.2 units/ml of penicillin, and 100 μg/ml streptomycin). The use of human ASM cells does not constitute human subjects research as all donor tissue is harvested anonymously and deidentified. All cells were maintained at 37°C in a humidified 5% CO$_2$ incubator. Cells were untransfected unless specifically noted.

Calcium Mobilization. Calcium mobilization was performed as previously described, with slight modifications (Luo et al., 2008). HEK293 cells or primary human ASM cells were grown to confluence in 15-cm dishes. Cells were treated with CellStripper (CellGro), washed, and concentrated to 5×10^6 cells/ml in Hank's balanced salt solution (HBSS) (CellGro) with 0.025% BSA. Fura-2 acetoxymethyl ester (Fura2-AM) (Life Technologies, Carlsbad, MA) dye was added to 2 μM, gently rocked, and incubated for 45 minutes at 37°C. Cells were pelleted by centrifugation, and the supernatant was replaced with 5 ml of HBSS and incubated at room temperature for 15 minutes to allow Fura2-AM processing. Cells were pelleted by centrifugation, washed, and resuspended at 30×10^6 cells/ml in ice-cold HBSS with 0.025% BSA. To measure calcium mobilization, 50,000 cells were incubated in HBSS without calcium and magnesium (CellGro) with 0.025% bovine serum albumin (BSA) in the presence or absence of various concentrations of P4pal-10 for 1 minute at 37°C. Cells treated with FR900359 were incubated on ice for 10 minutes before addition to the assay cuvette and 1-minute incubation at 37°C before the addition of agonists (final concentrations: 100 μM PAR1-AP, 100 μM carbachol, 100 nM bradykinin, 100 μM histamine, and 10 μM ATP; concentrations that promoted maximal calcium mobilization were used). Fura2-AM fluorescence was monitored using excitation at 340 and 380 nm and emission at 510 nm over a time course (LS55; PerkinElmer, Waltham, MA). Percent responsiveness was calculated as the fraction of peak response of the inhibitor-treated cells as compared with the response of the cognate ligand using cells not treated with an inhibitor.

G$_s$ Activation. HEK293 cells were plated in 24-well plates and grown to confluence in complete media. Before assaying, cells were treated with dimethylsulfoxide (DMSO) (0.5%), 100 nM FR900359, 10 μM P4pal-10, or 10 μM P4pal-10 Scr for 10 minutes at 37°C. Cells were stimulated with 100 nM isoproterenol for 10 minutes in the presence of 0.5 mM 3-isobutyl-1-methylxanthine (Sigma-Aldrich). Cells were lysed by the addition of 80 μl of 0.1 M HCl, followed by 20-minute incubation on an orbital shaker at room temperature. Lysates were cleared by centrifugation at 1000g for 10 minutes. cAMP levels were measured using the Cayman Chemical Cyclic AMP EIA kit following the manufacturer's instructions. Responsiveness was calculated as the percentage of isoproterenol-promoted cAMP produced as compared with the DMSO-treated cells.

G$_i$ Activation. HEK293 cells were plated in 24-well plates and grown to confluence in complete media. Before assaying, cells were treated with DMSO (0.5%), 100 nM FR900359, 10 μM P4pal-10, or 10 μM P4pal-10 Scr for 10 minutes at 37°C. In pertussis toxin–treated samples, cells were preincubated overnight with 100 ng/ml pertussis toxin at 37°C. Cells were treated for 1 minute with the agonist [50 nM Stromal-derived factor 1α for CXC chemokine receptor (CXCR) 4 experiments; 100 μM PAR1-AP for PAR1 experiments] before stimulation with 10 μM forskolin for 10 minutes. cAMP production was measured as described above. Responsiveness was calculated as the percentage of forskolin-promoted cAMP produced as compared with the DMSO-treated cells.

Gα_q Purification. Rat Gα_q and glutathione *S*-transferase (GST)-tagged Ric-8A were coexpressed from amplified, recombinant baculoviruses (2 and 8 ml, respectively) in 1 l of High-Five (Invitrogen, Carlsbad, MA) insect cell suspension culture for 48 hours. Insect cells were harvested and lysed in 20 mM HEPES, pH 8.0, 150 mM NaCl, 5 mM EDTA, 1 mM dithiothreitol (DTT), 11 mM CHAPS, 1 μM GDP, and protease inhibitor mixtures, as described (Chan et al., 2011a). GST-Ric-8A:Gα_q complexes were captured from the clarified lysates with glutathione Sepharose 4B (GE Healthcare, Pittsburgh, PA). The column was washed, and Gα_q was eluted slowly at 22°C with

20 mM HEPES, pH 8.0, 50 mM $MgCl_2$, 1 mM DTT, 11 mM CHAPs, 100 μM GDP, 10 mM NaF, 30 μM $AlCl_3$, and protease inhibitor mixtures. The $G\alpha_q$ was loaded onto a 1-ml Hi-Trap Q column (GE Healthcare) that had been equilibrated with 20 mM HEPES, pH 8.0, 1 mM EDTA, 1 mM DTT, and 11 mM CHAPS and eluted with a linear gradient to 500 mM NaCl in the same buffer. The $G\alpha_q$ Hi-Trap Q pool was concentrated using an Amicon Ultra-15 30,000 MWCO ultracentrifugal device (EMD Millipore, Billerica, MA) and gel filtered over a Superdex 200 HR10/300 column (GE Healthcare, Pittsburgh, PA) in 20 mM HEPES, pH 8.0, 100 mM NaCl, 1 mM EDTA, 1 mM DTT, 11 mM CHAPS, and 1 μM GDP. The $G\alpha_q$ was evaluated for purity by Coomassie-stained sodium dodecyl sulfate (SDS)-polyacrylamide gel electrophoresis (PAGE) and for activity using a Ric-8A-stimulated [^{35}S]guanosine 5′-O-[gamma-thio]triphosphate (GTPγS)-binding assay (Chan et al., 2011b).

Spontaneous GTPγS Binding. Intrinsic $G\alpha_q$ GTPγS binding measurements were performed as described (Nishimura et al., 2010). In brief, purified $G\alpha_q$ (500 nM) was preincubated with DMSO (0.5%), P4pal-10, or FR900359 for 5 minutes at 20°C in assay buffer (50 mM HEPES, pH 7.5, 1 mM EDTA, 1 mM DTT, 0.9 mM $MgSO_4$, and 0.05% Lubrol). Reactions were initiated by the addition of 10 μM [^{35}S]GTPγS (Perkin Elmer, Waltham, MA) and 300 mM $(NH_4)_2SO_4$. The reactions were stopped by the addition of 4 ml of ice-cold wash buffer (20 mM Tris-HCl, pH 7.5, 100 mM NaCl, and 2 mM $MgSO_4$), and the $G\alpha_q$ was captured by rapid filtration through BA85 nitrocellulose membranes (Millipore, Billerica, MA). The membranes were washed four times with 4 ml of ice-cold wash buffer, and [^{35}S]GTPγS binding was quantitated by liquid scintillation counting.

Detection of Active RhoA. GST–Rhotekin Rho-binding domain (RBD) (a generous gift from Dr. Philip Wedegaertner, Thomas Jefferson University, Philadelphia, PA) was expressed in *Escherichia coli* BL21 cells, which were grown at 37°C in 100 μg/ml ampicillin until the optical density reading at 600 nm was approximately 0.6 absorbance units. Protein expression was induced by the addition of 0.5 mM (final concentration) isopropyl β-D-1-thiogalactopyranoside and continued for 3 hours at 30°C. Cells were pelleted by centrifugation at 5000g for 15 minutes at 4°C and resuspended in 10 ml of STE buffer [10 mM Tris-HCl, pH 8.0, 100 mM NaCl, 1 mM EDTA, and 1 complete protease inhibitor tablet (Roche, Indianapolis, IN)]. One hundred microliters of 1 M DTT and 1.4 ml of 10% sarkosyl were added and mixed by inversion. The resuspension was sonicated for 1 minute and centrifuged at 18,000g for 30 minutes at 4°C. Four milliliters of 10% Triton X-100 was added to the supernatant, and the solubilized mixture was supplemented with STE buffer to 20 ml. One milliliter of glutathione sepharose beads, which were pre-equilibrated with Dulbecco's phosphate-buffered saline (DPBS), was added to the cleared lysate. GST-RBD loading occurred over 1-hour incubation at room temperature with gentle rocking. Glutathione sepharose beads were pelleted and washed three times with 50 ml of DPBS. The washed beads were suspended in DPBS, snap frozen, and stored at −80°C.

HeLa cells were grown in six-well plates to 60% confluence and transfected with FLAG-PAR1 for 48 hours prior to the experiment using X-tremeGENE 9 (Roche, Indianapolis, IN). Transfected HeLa cells were washed with DPBS and serum starved in Dulbecco's modified Eagle medium for 4 hours at 37°C. Ten minutes before stimulation, 10 μM P4pal-10, 100 nM FR900359, or 0.5% DMSO was added to the appropriate wells. After incubation, cells were stimulated with 100 μM PAR1-AP for 5 minutes at 37°C. On ice, stimulation media was removed and cells were lysed with 200 μl of lysis buffer [50 mM Tris-HCl, pH 7.5, 500 mM NaCl, 0.1% SDS, 0.5% deoxycholate, 1% Triton X-100, 20 mM $MgCl_2$, and 1 complete mini protease inhibitor tablet (Roche, Indianapolis, IN)]. Cells were scraped, briefly sonicated on ice, and centrifuged at 1000g for 10 minutes at 4°C. Five microliters of each lysate was saved for total RhoA analysis. Equal protein from each lysate was incubated with 40 μg of GST-RBD for 1 hour at 4°C. The beads were pelleted by centrifugation and washed twice with buffer (25 mM Tris-HCl, pH 7.5, 40 mM NaCl, 30 mM

$MgCl_2$, and 1 complete mini protease inhibitor tablet). Bound RhoA was eluted with 2× Laemelli buffer. Proteins were separated by SDS-PAGE on a 10% polyacrylamide gel, and activated RhoA pull down was analyzed by western blotting. RhoA was detected using a monoclonal RhoA antibody (1:1000; Santa Cruz Biotechnologies, Santa Cruz, CA) in Tris-buffered saline with Tween 20 (20 mM Tris-HCl, pH 7.5, 150 mM NaCl, and 0.1% Tween 20) (TBST) plus 5% BSA. Equal protein loading and RhoA expression was confirmed by blotting for RhoA after SDS-PAGE analysis of the initial lysates. For detection, western blots were incubated for 1 hour at room temperature with goat anti-mouse IRDye 800 conjugated (LI-Cor Biosciences, Lincoln, NE) antibodies at 1:2000. Detection of fluorescence was performed using an ODYSSEY infrared imaging system (LI-Cor Biosciences).

Airway Smooth Muscle Growth. Primary human airway smooth muscle cells were plated at a density of 10,000 cells per well on a 96-well white opaque plate precoated with poly-L-lysine in complete media. After 24 hours, the complete media was removed and the cells were washed once with DPBS. Each well was supplemented with 100 μl of media (Ham's F12 medium, 25 mM HEPES, 1.7 mM $CaCl_2$, 2 mM L-glutamine, 0.2 units/ml of penicillin, 100 μg/ml streptomycin, 5 μg/ml apo-transferrin, 1 μM insulin, and 100 μM ascorbic acid) and incubated for 48 hours at 37°C. The media was removed, and cells were incubated with DMSO (0.5%), 10 μM P4pal-10, or 100 nM FR900359 for 30 minutes in serum-free ASM media (Ham's F12 medium, 25 mM HEPES, 1.7 mM $CaCl_2$, 2 mM L-glutamine, 0.2 units/ml of penicillin, and 100 μg/ml streptomycin). At 30 minutes, cells were treated with vehicle (serum-free ASM media), 1 U/ml thrombin, 10 nM epidermal growth factor (EGF) (Sigma-Aldrich), or a thrombin/EGF combination for 24 hours. Media was then removed, and each well was incubated with 100 μl of WFI water (CellGro) for 1 hour at 37°C. One hundred microliters of 2× Pico Green Mix (Invitrogen) was added to each well, and cells were incubated in the dark for 1 hour at room temperature. Pico green fluorescence was excited at 485 ± 20 nm, and emission was monitored at 515 ± 25 nm on a Tecan Infinite F500 microplate reader (Tecan, Männedorf, Switzerland).

AKT Phosphorylation. Primary human ASM cells were grown to 70–80% confluence in six-well plates in complete media. Cells were starved for 24 hours in serum-free media. Ten minutes prior to stimulation, cells were treated with DMSO (0.5%), 10 μM P4pal-10, or 100 nM FR900359. Cells were stimulated with vehicle (serum-free ASM media), 1 U/ml thrombin, 10 nM EGF, or a thrombin/EGF combination for 6 hours at 37°C. On ice, cells were lysed by the addition of 200 μl of lysis buffer (20 mM HEPES, pH 7.2, 150 mM NaCl, 10 mM EDTA, 1% Triton X-100, and 1 complete protease inhibitor tablet) and brief sonication. The 5× Laemelli buffer was added, and samples were boiled for 5 minutes. Samples were separated by SDS-PAGE on a 10% polyacrylamide gel, and AKT phosphorylation was analyzed by western blotting. AKT phosphorylation was detected using a phosphospecific antibody (1:1000) against AKT phospho-serine 473 (Cell Signaling Technology, Danvers, MA) in TBST with 5% BSA. Equal AKT expression was confirmed by stripping the blot and reprobing using rabbit polyclonal anti-AKT (Cell Signaling Technology) at 1:1000 in TBST with 5% BSA. For detection, western blots were incubated for 1 hour at room temperature, with both goat anti-rabbit IRDye 680 conjugated (LI-Cor Biosciences) and goat anti-mouse IRDye 800 conjugated (LI-Cor Biosciences) antibodies at 1:2000. Detection of fluorescence was performed using the ODYSSEY infrared imaging system (LI-Cor Biosciences).

Preparation of Precision Cut Lung Slices. Human precision cut lung slices were prepared from donor lungs unsuitable for transplantation in accordance with the Institutional Review Board at the University of Pennsylvania as previously described (Cooper and Panettieri, 2008; Cooper et al., 2011). Briefly, whole human lungs from nonasthma donors with no known chronic illness or medication use were dissected and inflated using 2% (w/v) low melting point agarose. Once the agarose set, the lobe was sectioned, and cores with 8-mm diameters were made. The cores that contained a small airway

by visual inspection were sliced at a thickness of 350 μm (VF300 Vibratome; Precisionary Instruments, Greenville, NC) and collected in wells containing supplemented Ham's F-12 medium. Suitable airways ($\leq$1 mm in diameter) on slices were selected on the basis of the following criteria: presence of a full smooth muscle wall, presence of beating cilia, and unshared muscle walls at airway branch points to eliminate possible counteracting contractile forces. Each slice contained ~98% parenchyma tissue; hence, all airways situated on a slice had sufficient parenchymal tissue to impart basal tone. Adjacent slices containing contiguous segments of the same airway were paired and served as controls and were incubated at 37°C in a humidified air–CO$_2$ (95–5%) incubator. Sections were placed in fresh media every 2 to 3 hours during the remainder of *day 1* and all of *day 2* to remove the released agarose and endogenous substances that variably confound the production of inflammatory mediators and/or alter airway tone.

Precision Cut Lung Slice Bronchoconstriction Measurements. To assess the luminal area, lung slices were placed in a 12-well plate in media and held in place using a platinum weight with nylon attachments. The airway was located using a microscope (Nikon Eclipse; model number TE2000-U; magnification, ×40; Chiyoda, Tokyo, Japan) connected to a live video feed [Evolution QEi; model number 32-0074A-130 video recorder (Media Cybernetics, Rockville, MD)]. The airway luminal area was measured using Image-Pro Plus software (version 6.0; Media Cybernetics, Rockville, MD) and represented in units of square micrometers (Cooper and Panettieri, 2008; Cooper et al., 2011). After functional studies, the area of each airway at baseline and for each dose of agonist was calculated using Image-Pro Plus software.

Lung slices were pretreated with FR900359 (0.1 or 1 μM), P4pal-10 (20 μM), or P4pal-10 Scr (20 μM) for 30 minutes at 37°C. Slices were then bronchoconstricted to a dose response of carbachol or histamine (10^{-8} to 10^{-4} M). The luminal area was measured, and sigmoidal dose response curves were generated from the data. Maximal bronchoconstriction (E_{max}), sensitivity of the airways to the contractile agonist − log of the effective concentration to induce 50% bronchoconstriction (log EC$_{50}$), and the integrated response to the contractile agonist – area under the curve were calculated from the dose response curves that were generated and compared.

Magnetic Twisting Cytometry. Dynamic changes in cell stiffness were measured in isolated human ASM using forced motions of functionalized beads anchored to the cytoskeleton through cell surface integrin receptors, as previously described in detail (Fabry et al., 2001; An et al., 2006; Deshpande et al., 2010). The increase or decrease in stiffness is considered an index of single-cell smooth muscle contraction and relaxation, respectively. For these studies, serum-deprived, postconfluent cultured ASM cells were plated at 30,000 cells/cm^2 on plastic wells (96-well Removawell, Immulon II; Dynatec Labs, El Paso, TX) previously coated with type I collagen (VitroCol; Advanced BioMatrix, Inc., San Diego, CA) at 500 ng/cm^2, and maintained in serum-free media for 24 hours at 37°C in humidified air containing 5% CO$_2$. These conditions have been optimized for seeding cultured cells on collagen matrix and for assessing their mechanical properties (Fabry et al., 2001; An et al., 2006; Deshpande et al., 2010). For each individual cell, the baseline stiffness was measured for the first 60 seconds, and after drug addition, the stiffness was measured continuously for the next 240 seconds. Drug-induced changes in cell stiffness approached a steady-state level by 240 seconds. Unless otherwise stated, ASM cells were pretreated for 5 minutes with 3 μM pepducin. The effects of the inhibitors were normalized to respective steady-state drug effects (without inhibitors).

Results

P4pal-10 Is an Antagonist of Multiple G$_q$-Coupled Receptors. P4pal-10 is a 10 amino acid pepducin derived from the third intracellular loop of PAR4 and was previously shown to inhibit G$_q$ signaling from PAR4, PAR1, and the TXA$_2$R (Covic et al., 2002; Stampfuss et al., 2003). To assess whether P4pal-10 broadly inhibits G$_q$ signaling, we monitored agonist-promoted calcium mobilization from endogenous GPCRs in HEK293 cells and primary human ASM cells. P4pal-10 effectively inhibits responsiveness to a number of agonists, including carbachol, bradykinin, histamine, and ATP, with potencies that range from 0.24 μM (bradykinin) to 7.4 μM (ATP) (Fig. 1, A and B). To examine if P4pal-10 was specific for G$_q$-coupled GPCRs, the ability to inhibit G protein activation from the β_2-adrenergic receptor (β_2AR) (G$_s$ coupled) and CXCR4 (G$_i$ coupled) was also assessed. P4pal-10 was unable to modulate cAMP production from β_2AR (Fig. 1C) or adenylyl cyclase inhibition from CXCR4 (Fig. 1D). Thus, it appears that P4pal-10 operates through a specific subset of G$_q$-coupled receptors and does not act as a broad antagonist for G protein–receptor coupling.

P4pal-10 Inhibits Cognate G Protein Coupling to PAR1, whereas FR900359 Directly Inhibits G$_q$ Activation. It is plausible that P4pal-10 could operate by selectively inhibiting G$_q$ activation in a receptor-dependent manner or by directly inhibiting activation of G$_q$. To dissect these potential mechanisms of action, the ability to modulate spontaneous nucleotide exchange was assessed using purified Gα_q. P4pal-10 had little effect on the rate of nucleotide exchange of Gα_q, suggesting that it does not operate by directly restraining G$_q$ dynamics (Fig. 2A). We also evaluated the effects of the G$_q$ inhibitor FR900359 and, as expected, FR900359 effectively inhibits GTPγS incorporation and corroborates the similarities with YM-254890.

PAR1 is a protease-activated receptor that, when stimulated by thrombin or an exogenous peptide ligand, couples to G$_q$, G$_i$, and G$_{12/13}$ (Fig. 2B) (Gilchrist et al., 2001). As PAR1 couples to multiple G proteins and is sensitive to P4pal-10 (Fig. 1A), it serves as a good model to further dissect the mechanism of P4pal-10 inhibition. In a receptor-dependent model, P4pal-10 might operate by selectively inhibiting G$_q$ coupling to PAR1 or by inhibiting cognate G$_q$, G$_i$, and G$_{12/13}$ coupling to PAR1. To study the ability of P4pal-10 and FR900359 in isolation, the cognate signaling from each G protein subtype was assessed in cells. Both FR900359 and P4pal-10 can inhibit PAR1-AP stimulated calcium mobilization, an event typically associated with G$_q$ activation (Fig. 2C). Activation of G$_i$ decreases cAMP production due to inhibition of adenylyl cyclase activity (Bokoch et al., 1984). PAR1-mediated G$_i$ coupling resulted in an ~40% decrease in forskolin-stimulated cAMP production. Cells pretreated with P4pal-10 were unable to modulate forskolin-stimulated cAMP production similarly to cells pretreated with pertussis toxin, a well characterized inhibitor of G$_i$ activation (Fig. 2D). The scrambled control pepducin had no effect on adenylyl cyclase inhibition, whereas FR900359 also did not alter G$_i$ function as it is a G$_q$-specific inhibitor (Fig. 2D). PAR1 also couples to G$_{12/13}$ activity, which can be monitored through the detection of activated RhoA (McLaughlin et al., 2005). When active, RhoA binds GTP and undergoes a conformational change that can be detected by binding to GST-RBD. Using this assay, PAR1-AP effectively stimulated RhoA activation in HEK293 cells (Fig. 2E). Cells pretreated with P4pal-10 demonstrated a significant loss of detectable GTP-RhoA that was not observed in cells treated with FR900359 or P4pal-10 Scr (Fig. 2E). Using PAR1 as a model receptor, it appears that P4pal-10 may operate by inhibiting all cognate G protein coupling to a sensitive receptor, such as PAR1,
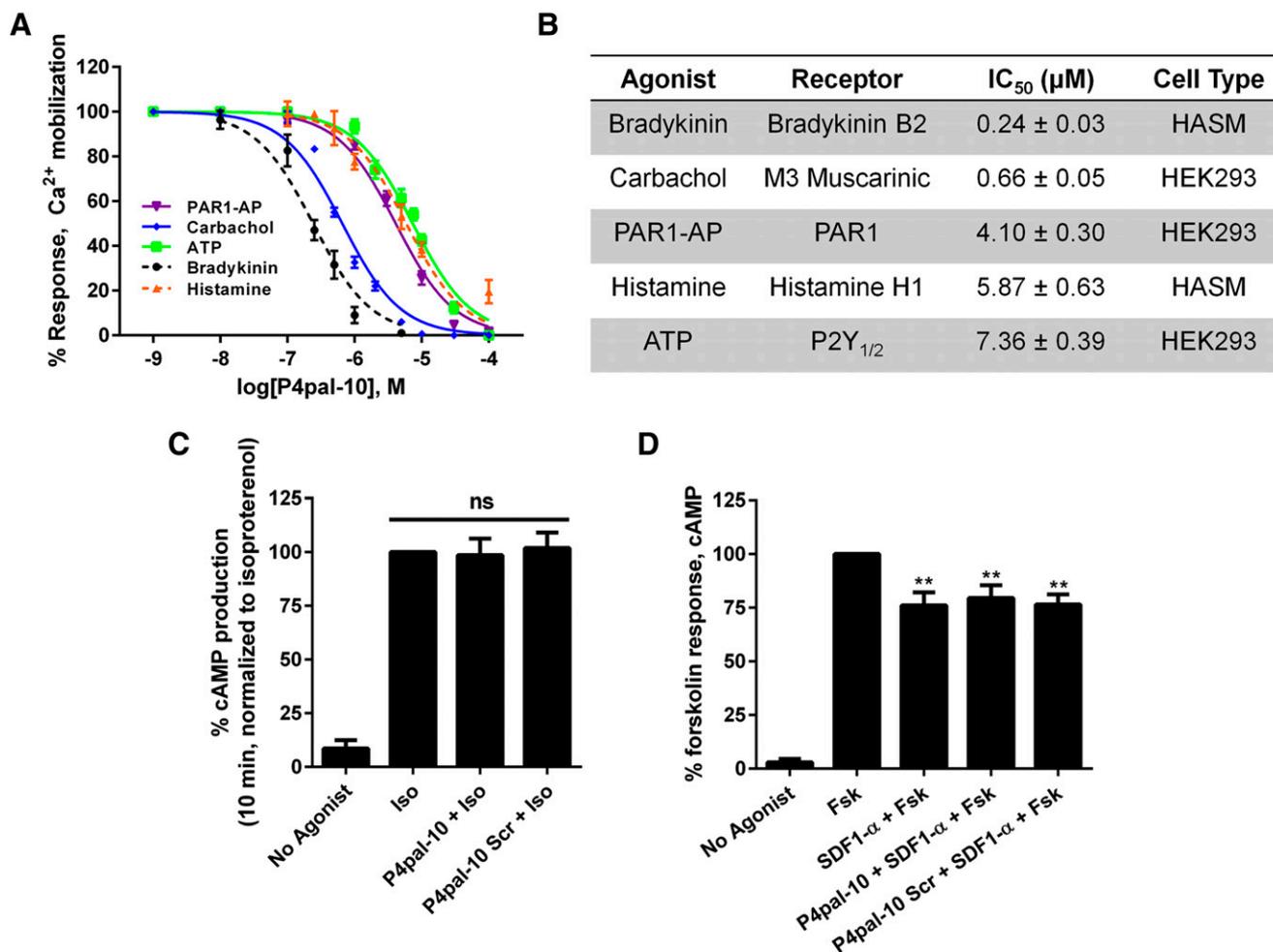
Fig. 1. P4pal-10 is an antagonist of multiple G_q-coupled receptors. (A) Agonist-promoted calcium mobilization was monitored by Fura-2 AM fluorescence in HEK293 and HASM cells pretreated for 1 minute with various concentrations of P4pal-10. Peak fluorescence values are reported. (B) P4pal-10 IC_{50} values are reported for responsiveness to various G_q-coupled receptor agonists. (C) Ten micromolars of P4pal-10 does not inhibit isoproterenol-stimulated cAMP production (G_s mediated) in HEK293 cells. The data are represented by the mean ± S.D. from three independent experiments; ns, not significant. (D) Ten micromolars of P4pal-10 does not inhibit SDF-1α–stimulated adenylyl cyclase inhibition (G_i mediated) in HEK293 cells. The data are represented by the mean ± S.D. from three independent experiments. **$P < 0.01$ versus forskolin-treated cells using a two-way unpaired t test.

whereas FR900359 effectively inhibits G_q activation but does not alter receptor-stimulated activation of G_i or $G_{12/13}$.

Inhibition of G_q Activation by P4pal-10 or FR900359 Effectively Prevents Synergistic Airway Smooth Muscle Growth. Pathophysiologic advancement of chronic asthma includes the physical occlusion of the airway lumen by remodeling mechanisms, such as ASM hyperplasia/hypertrophy (Al-Muhsen et al., 2011). In vitro models of ASM growth using isolated primary human ASM cells have established a synergistic relationship between the growth effects of receptor tyrosine kinase ligands, such as EGF and platelet-derived growth factor, and concurrent exposure to G_q-coupled receptor ligands (Ediger and Toews, 2000; Krymskaya et al., 2000; Gosens et al., 2003; Billington et al., 2005; Kong et al., 2006). Synergistic ASM cell growth is dependent on the activation of G_q-coupled GPCRs and operates independently of G_i activation (insensitive to pertussis toxin) and $G_{12/13}$ signaling (insensitive to p115RhoGEF-mediated $G_{12/13}$ inactivation) (Kong et al., 2006). As G_q plays a central role in this phenomenon, it is plausible that the inhibition of G_q activation could decouple the synergistic growth response from typical responsiveness to receptor

tyrosine kinase–dependent growth factors. To examine this, primary human ASM cells were growth arrested and exposed to thrombin (1 U/ml), EGF (10 nM), or cotreatment (thrombin + EGF) in the presence or absence of P4pal-10 or FR900359. As expected, ASM cells showed modest growth when treated with thrombin; more pronounced growth in the presence of EGF; and synergistic growth when cotreated with thrombin and EGF (Fig. 3A). FR900359 effectively inhibited the synergistic growth effect of thrombin + EGF treatment to levels comparable to EGF stimulation alone, whereas cellular responsiveness to EGF was unaltered. P4pal-10 mirrored the pharmacological profile of FR900359, whereas P4pal-10 Scr had no effect on ASM growth (Fig. 3A).

The activation of G_q-coupled GPCRs leads to the activation of myriad intracellular signaling pathways that can contribute to cell growth. Interestingly, the synergy between G_q-coupled receptor agonists operates primarily through $G\beta\gamma$-dependent activation of Akt and downstream targets of Akt, particularly P70 S6 kinase (Ediger and Toews, 2000; Krymskaya et al., 2000; Kong et al., 2006). Inhibition of Src, Rho, and Rho kinase along with knockdown of β-arrestin suggests no role for these signaling pathways in synergistic
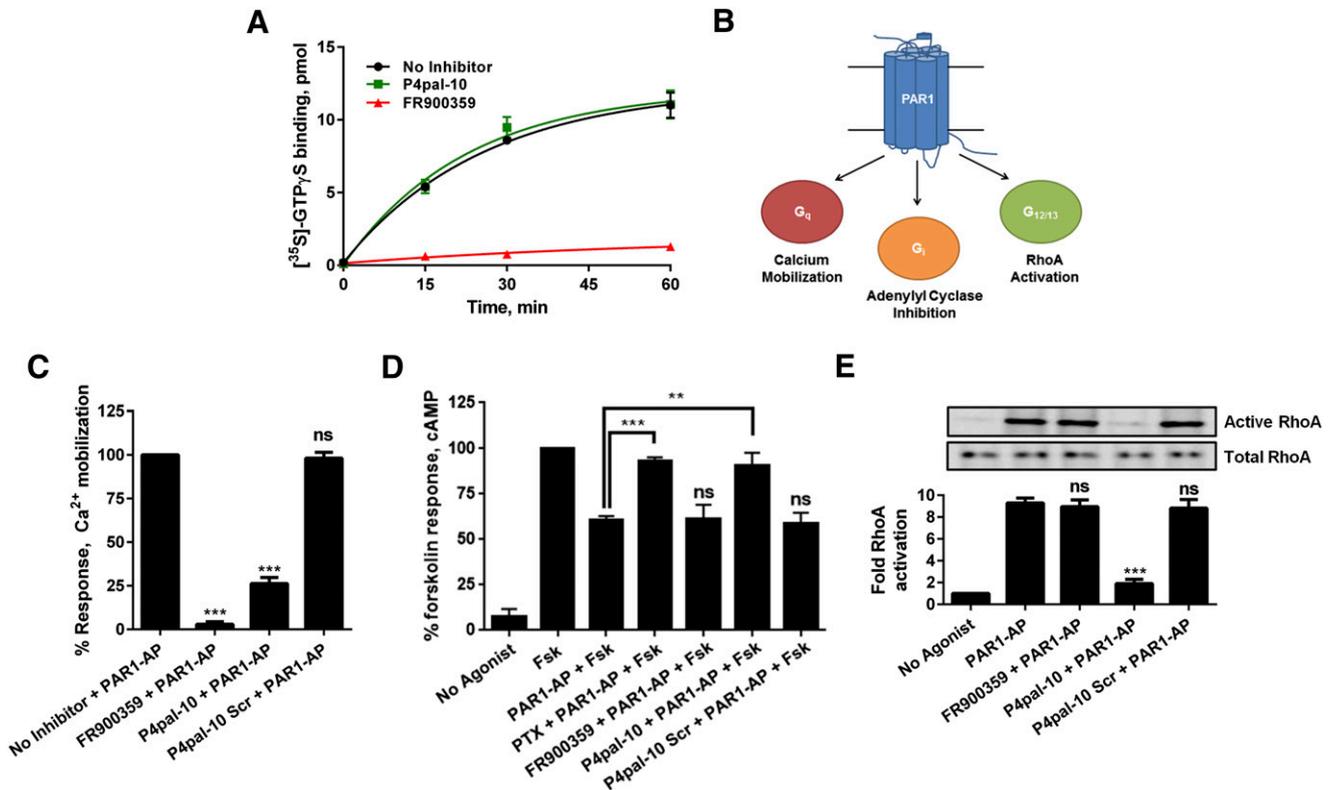
Fig. 2. P4pal-10 inhibits cognate G protein coupling to PAR1, whereas FR900359 directly inhibits G_q. (A) One hundred nanomolars of FR900359, but not 10 μM P4pal-10, interdicts spontaneous GTPγS binding to purified $G\alpha_q$. The data are represented by the mean $\pm$ S.D. from three independent experiments. (B) PAR1 can couple to G_q (measured by calcium mobilization), G_i (measured by adenylyl cyclase inhibition), and $G_{12/13}$ (measured by RhoA activation). (C) Ten micromolars of P4pal-10 and 100 nM of FR900359 inhibit PAR1-AP–promoted calcium mobilization. ns, not significant. ***$P < 0.001$ versus vehicle-treated cells using a two-way unpaired t test. (D) Ten micromolars of P4pal-10, but not 100 nM FR900359 or 10 μM P4pal-10 Scr, can inhibit PAR1-dependent G_i activation. P4pal-10 exhibited comparable efficacy to pertussis toxin, an inhibitor of G_i activation. The data are represented by the mean $\pm$ S.D. from three independent experiments. **$P < 0.01$ and ***$P < 0.001$ versus PAR1-AP–treated cells using a two-way unpaired t test. (E) Ten micromolars of P4pal-10, but not 100 nM FR900359 or 10 μM P4pal-10 Scr, can inhibit PAR1-AP–stimulated $G_{12/13}$ activation. The data are represented by the mean $\pm$ S.D. from three independent experiments. ***$P < 0.001$ versus PAR1-AP–treated cells using a two-way unpaired t test.

ASM growth (Kong et al., 2006). G$\beta\gamma$ promotes AKT activation by direct phosphatidylinositol-3-kinase recruitment, phosphoinositide-dependent kinase-1 activation, and AKT-T308 phosphorylation by phosphoinositide-dependent kinase-1 (Billington et al., 2005). As for Gα_q, the signaling cascade that activates AKT is not as well established in ASM. Similar to the phenotypic growth assays, growth-arrested primary human ASM cells were treated in the presence or absence of P4pal-10 or FR900359, with thrombin (1 U/ml), EGF (10 nM), or thrombin and EGF. Using an AKT-phosphospecific antibody detecting phosphorylation at S473, an indicator of activation, cells exhibited synergistic phosphorylation at S473 when costimulated with thrombin and EGF (Fig. 3B). Both FR900359 and P4pal-10 effectively inhibited synergistic responsiveness to levels comparable to cells treated with EGF alone. P4pal-10 Scr had little effect on agonist-promoted AKT phosphorylation (Fig. 3B).

FR900359, but Not P4pal-10, Can Interdict Broncho-constriction in Human Precision Cut Lung Slices. Airway hyperresponsiveness and amplified ASM shortening define the asthmatic diathesis. ASM contraction is mediated through myosin light chain phosphorylation downstream of G_q activation (Hakonarson and Grunstein, 1998). Parasympathetic stimulation of airway contraction is primarily mediated through the M_3 muscarinic acetylcholine receptor (Canning and Fischer, 2001). However, it is known that activation of

multiple G_q-coupled GPCRs, including PARs and histamine receptors, can feed into the dynamics of airway contraction (Deshpande and Penn, 2006). Current therapeutic approaches may include the use of muscarinic or leukotriene receptor antagonists to attenuate the relative contribution of these receptors to the contractile state (Bel, 2013). Conceivably, due to the heterologous nature of the signaling inputs that regulate airway contraction, a molecule that inhibits multiple G_q-coupled receptors, such as P4pal-10, or a molecule that directly inhibits G_q activation, such as FR900359, may offer unique therapeutic benefits.

P4pal-10 and FR900359 inhibited the activation of G_q-dependent processes, such as calcium mobilization or synergistic ASM growth. However, these assays were performed with either suspended cells or ASM cells grown in a monolayer. As ASM in situ is situated under a layer of epithelial cells in the airway, the therapeutic potential of P4pal-10 and FR900359 in the context of a bronchial tissue was studied using human precision cut lung slices. As an ex vivo model of airway dynamics, precision cut lung slices remain responsive to multiple receptor agonists and have been used to study physiologic processes, including airway bronchoconstriction. Preincubation with 100 nM or 1 μM FR900359 shifted the EC_{50} of carbachol-promoted airway contraction by 2- or 11-fold, respectively, and promoted a large reduction in maximal bronchoconstriction at 1 μM FR900359 (Fig. 4, A

A
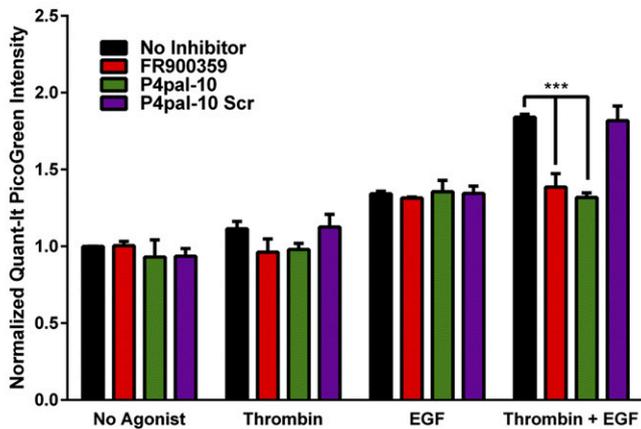
B
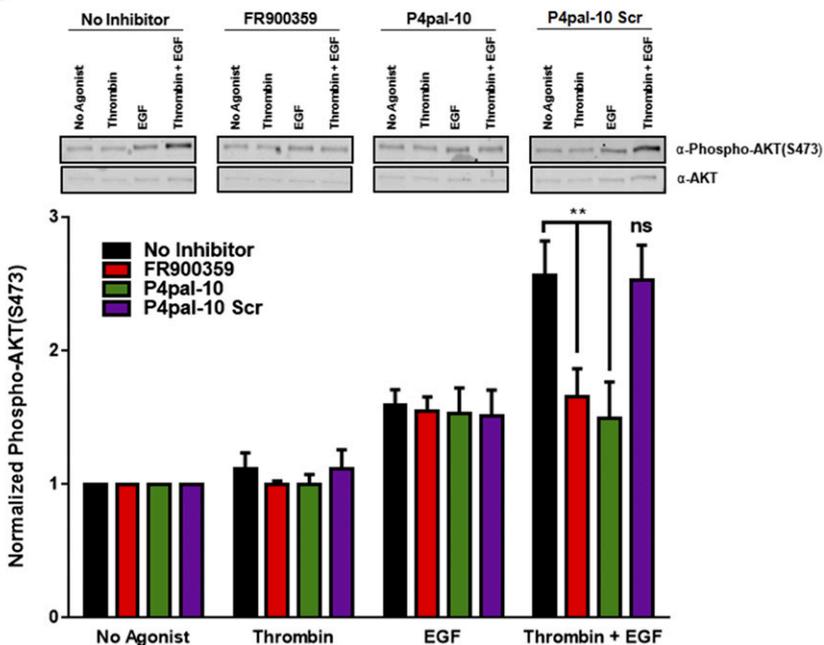
Fig. 3. Inhibition of G_q-activation by P4pal-10 or FR900359 effectively inhibits synergistic HASM growth and growth signaling. (A) Ten micromolars of P4pal-10 or 100 nM FR900359, but not P4pal-10 Scr, can significantly inhibit synergistic human ASM growth in response to EGF and thrombin cotreatment while not modulating EGF-promoted cell growth. Cell growth was monitored 24 hours poststimulation using a PicoGreen fluorescence assay. The data are represented by the mean ± S.D. of three independent experiments. ***$P < 0.001$ versus vehicle-treated cells using a two-way unpaired t test. (B) Ten micromolars of P4pal-10 or 100 nM FR900359, but not P4pal-10 Scr, can significantly inhibit synergistic Akt phosphorylation at S473 in response to EGF and thrombin cotreatment while not modulating EGF-promoted phosphorylation. AKT-S473 phosphorylation was assessed by western blot 6 hours poststimulation. The data are represented by the mean ± S.D. of three independent experiments. ns, not significant. **$P < 0.01$ versus vehicle-treated cells incubated with thrombin and EGF using a two-way unpaired t test.

and C), whereas P4pal-10 was ineffective at modulating contractile responsiveness to carbachol stimulation (Fig. 4, B and C). Airway contraction was also assessed in response to histamine. As expected, FR900359 was able to effectively inhibit contractile responsiveness to high concentrations of histamine, with EC_{50} shifts >50-fold and a large reduction in maximal bronchoconstriction (Fig. 4, D and F). Interestingly, P4pal-10 shifted the EC_{50} of histamine responsiveness by 8-fold, albeit with a minimal effect on maximal bronchoconstriction, whereas P4pal-10 Scr had little effect on the EC_{50} (Fig. 4, E and F). Although it is expected that P4pal-10 would have the properties to interdict carbachol and histamine-promoted airway contraction, we observed relatively weak inhibition of these processes as compared with FR900359 (Fig. 4, C and E). In the airway, the smooth muscle is situated under a layer of epithelial cells that P4pal-10 would have to bypass or transverse to access the ASM.

To more directly assess the ability of P4pal-10 to inhibit isolated ASM cell contraction, magnetic twisting cytometry was used to assay single cell contraction. P4pal-10 effectively inhibited carbachol and histamine-promoted single cell ASM contraction while having no effect on isoproterenol-promoted relaxation (Fig. 4, F–H). Additionally, P4pal-10 Scr did not exhibit any significant effects on agonist-promoted single cell contraction or relaxation (Fig. 4, F–H). As P4pal-10 was able to inhibit agonist-promoted contraction in isolated ASM cells but did not exhibit similar efficacy in the precision cut lung slice model, tissue accessibility may be limiting the therapeutic efficacy of P4pal-10 in the airway.

Discussion

Asthma, a complex airway syndrome, manifests as airway hyperresponsiveness and inflammation due to multiple environmental and signaling inputs, resulting in the exclusion of the airway lumen. G_q plays a central role in the pathophysiology of airway disease and mediates ASM contractility, airway remodeling, and ASM cell growth (Deshpande and Penn, 2006). To assess the effects of broadly inhibiting G_q activation, we examined a receptor-dependent pepducin antagonist of G_q activation alongside a small-molecule, direct inhibitor of G_q activation.
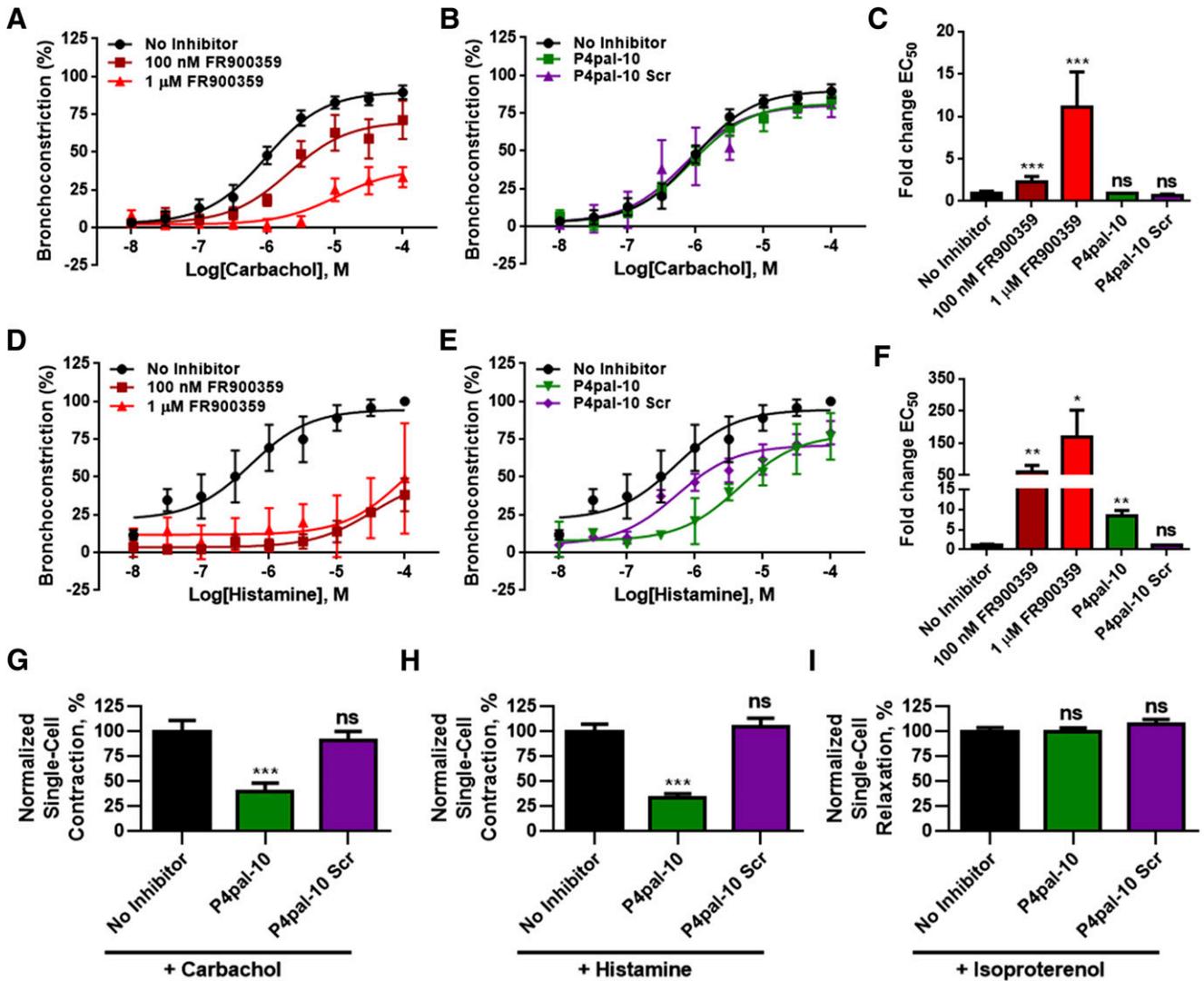
Fig. 4. FR900359, but not P4pal-10, can inhibit airway contraction in human precision cut lung slices. (A) One hundred nanomolars and 1 μM FR900359 inhibited carbachol-promoted airway contraction. The data are represented by the mean ± S.E.M. of four independent experiments and fitted to a sigmoidal dose-response model. (B) P4pal-10 and P4pal-10 Scr had no effect on airway contraction in response to carbachol. The data are represented by the mean ± S.E.M. of four independent experiments and fitted to a sigmoidal dose-response model. The no inhibitor curve is derived from the same data set in both (A and B). (C) One hundred nanomolars or 1 μM of FR900359 shifted the estimated EC$_{50}$ value of carbachol-promoted airway contraction by 2- and 11-fold, respectively. P4pal-10 and P4pal-10 Scr did not modulate carbachol responsiveness. The data are represented by the mean ± S.E.M. of four independent experiments. ns, not significant. ***$P < 0.001$ versus vehicle-treated tissue using a two-way unpaired t test. (D) One hundred nanomolars and 1 μM of FR900359 effectively inhibited histamine-promoted airway contraction. The data are represented by the mean ± S.E.M. of three independent experiments and fitted to a sigmoidal dose-response model. (E) P4pal-10 partially inhibited airway contraction in response to histamine. The data are represented by the mean ± S.E.M. of three independent experiments and fitted to a sigmoidal dose-response model. The no inhibitor curve is derived from the same data set in both (D and E). (F) P4pal-10 shifted the estimated EC$_{50}$ value of histamine-promoted airway contraction by 8-fold, whereas 100 nM and 1 μM FR900359 shifted the EC$_{50}$ > 50-fold. The data are represented by the mean ± S.E.M. of three independent experiments. *$P < 0.05$ and **$P < 0.01$ versus vehicle-treated tissue using a two-way unpaired t test. (G) Magnetic twisting cytometry analysis of isolated ASM dynamics shows that pretreatment with 3 μM P4pal-10 ($n = 232$) significantly inhibited carbachol-promoted single-cell contraction as compared with no inhibitor/vehicle treatment ($n = 331$). P4pal-10 Scr did not exhibit similar efficacy ($n = 266$). The data sets are normalized to no inhibitor/vehicle treatment. ***$P < 0.001$ compared with vehicle-treated cells using a one-way analysis of variance (ANOVA) analysis. (H) Magnetic twisting cytometry analysis of isolated ASM dynamics shows that pretreatment with 3 μM P4pal-10 ($n = 867$) significantly inhibited histamine-promoted single-cell contraction as compared with no inhibitor/vehicle treatment ($n = 692$). P4pal-10 Scr did not exhibit similar efficacy ($n = 486$). The data sets are normalized to no inhibitor/vehicle treatment. ***$P < 0.001$ compared with vehicle-treated cells using a one-way ANOVA analysis. (I) Magnetic twisting cytometry analysis of isolated ASM dynamics shows that pretreatment with 3 μM P4pal-10 ($n = 418$) or P4pal-10 Scr ($n = 292$) did not modulate isoproterenol-promoted single-cell relaxation as compared with no inhibitor/vehicle treatment ($n = 569$). The data sets are normalized to no inhibitor/vehicle treatment. ns, not significant compared with vehicle-treated cells using a one-way ANOVA analysis.

P4pal-10 is a pepducin antagonist derived from intracellular loop 3 of PAR4. In the initial report, P4pal-10 exhibited strong inhibition of PAR4-mediated platelet aggregation, with an IC$_{50}$ of ~0.5–1 μM, and, interestingly, was able to also modulate PAR1-mediated platelet aggregation (Covic et al., 2002). P4pal-10 could also inhibit G$_q$ signaling in response to

TXA$_2$R stimulation (Stampfuss et al., 2003), although this effect was not observed by Covic et al. (2002). By monitoring calcium mobilization in HEK293 and human ASM cells, P4pal-10 inhibited a number of G$_q$-coupled receptors, with IC$_{50}$ values ranging from 0.24 to 7.4 μM. As the efficacy of P4pal-10 varied greatly, depending on the agonist specificity,

it seems unlikely that P4pal-10 is directly sequestering G_q and preventing receptor interaction. Indeed, P4pal-10 did not modulate nucleotide exchange using purified $G\alpha_q$. An interesting property exhibited by P4pal-10 concerns the ability to interdict all G protein coupling to a single receptor. PAR1 can couple to G_q, G_i, and $G_{12/13}$, all of which can be inhibited by P4pal-10. It is unknown at this time if P4pal-10 operates by restricting conformational dynamics of its targeted receptors to stabilize an inactive state or if it prevents receptor interaction with a G protein.

As P4pal-10 appears to operate through the receptor, the mechanism in which P4pal-10 inhibits a diverse set of G_q-coupled receptors remains elusive. It was previously believed that pepducins operate through the cognate receptor from which they were derived (O'Callaghan et al., 2012); however, some pepducins, including P4pal-10, exhibit efficacy across multiple receptor subtypes (Stampfuss et al., 2003; Carr et al., 2014). Although many of these receptors do not share significant sequence similarity, many of the P4pal-10 sensitive receptors share strong, sequential homology with the N-terminal half of the P4pal-10 sequence (SGRRYG). Some receptors that were characterized as P4pal-10 insensitive, such as β_2AR, may share some sequence homology with P4pal-10, but these regions of similarity are either short and highly disjointed or found in receptor regions that are likely not playing a role in P4pal-10 function (extracellular loops and transmembrane domains). Further, P4pal-10–sensitive receptors exhibited sequence homology with P4pal-10 in the intracellular domains of the receptor, along with some portions of transmembrane domains that border the intracellular surface. With this in mind, P4pal-10 may interrupt critical intrareceptor or receptor–G protein contacts that are necessary for agonist-promoted G protein activation. As each receptor has distinct differences in receptor sequence, the spectrum of P4pal-10 sensitivity (Fig. 1, A and B) may be attributed to the degree of similarity between the receptor and P4pal-10 or the unknown P4pal-10 interaction site.

FR900359, also known as UBO-QIC, was first reported as a methanol-extracted natural compound isolated from *Ardisia crenata sims* that was proposed to inhibit in vitro platelet aggregation and decrease blood pressure in rats (Fujioka et al., 1988). Similar to the well studied YM-254890, FR900359 directly inhibited in vitro spontaneous nucleotide exchange using purified $G\alpha_q$, which suggests that it is operating by constraining G_q conformational dynamics. Our studies confirmed the proposed specificity of the compound at concentrations that were 10 times higher than those previously studied in vitro. FR900359 did not modulate G_s, G_i, or $G_{12/13}$ signaling while strongly inhibiting G_q activation (Inamdar et al., 2015). As many GPCRs couple to multiple G proteins, the use of an inhibitor with defined specificity can effectively bias signaling from a GPCR. Most often studied is the ability of a GPCR agonist to promote a biased signal, but FR900359 promotes an inhibitor-biased signal by selectively eliminating the activation of a particular intracellular signaling protein. Using PAR1, for example, FR900359 effectively eliminated G_q activation from PAR1 while allowing activation of G_i and $G_{12/13}$ from the same receptor. Thus, FR900359 changed PAR1 signaling from G_q, G_i, and $G_{12/13}$ to only G_i and $G_{12/13}$. The concept of inhibitor biased signaling can be applied to a number of kinase inhibitors (e.g., G protein–coupled receptor kinase, protein kinase A, and protein kinase C) or molecular inhibitors (pertussis toxin, Rho inhibitors,

etc.) to modulate the lifetime (kinetics) or efficacy of signaling and thus provide a new dimension to biasing intracellular signaling pathways.

Investigation into the molecular mechanisms of airway disease clearly demonstrates a central role for G_q activation and downstream signaling. Most prominently in patients with asthma, hyper-responsiveness of ASM by phosphorylation of the myosin light chain is, in part, a downstream consequence of G_q-promoted calcium mobilization (Hakonarson and Grunstein, 1998). Although the mechanism of elevated G_q signaling remains incompletely understood, it is believed that increased parasympathetic activation of the airway, along with a local increase in G_q-coupled receptor agonists (e.g., thrombin, histamine, and ATP) enhances the contractile state of the asthmatic airway. It is suspected that both inputs contribute to the pathology as muscarinic antagonists only partially alleviate airway tension in patients (Bel, 2013). Using ex vivo human precision cut lung slices, direct inhibition of G_q activation by FR900359 was able to significantly impact airway contraction. Thus, it is conceivable that the use of a G_q-specific inhibitor may be an advantageous approach to the complex nature of treating bronchoconstriction in the asthmatic airway.

G_q also contributes to airway remodeling, including ASM growth, which physically occludes the lumen of the airway (Al-Muhsen et al., 2011). ASM proliferation is exacerbated in the disease state due to multiple factors, including the increased presence of G_q-coupled receptor agonists, such as histamine, acetylcholine, thromboxane, leukotriene D4, serotonin, and ATP, in the airway (Deshpande and Penn, 2006). In vitro models of ASM growth have established a synergistic relationship between the growth effects of receptor tyrosine kinase ligands, such as EGF and platelet-derived growth factor, and concurrent exposure to G_q-coupled receptor ligands, which is mediated through the activation of Akt and the P70 S6 kinase (Ediger and Toews, 2000; Krymskaya et al., 2000; Kong et al., 2006). Both P4pal-10 and FR900359 inhibited synergistic ASM growth and synergistic AKT activation with similar efficacy. These compounds, through fundamentally different mechanisms, inhibit synergy without modulating cellular responsiveness to an receptor tyrosine kinase growth factor further corroborates the critical role G_q plays in this phenomena and pathology. G_q can also promote the release of inflammatory factors, such as cytokines (Fujii et al., 1998; Fujii and Kawashima, 2000). Considering the data monitoring ASM contractility and growth, it would be expected that both P4pal-10 and FR900359 may have a significant impact on the efficacy of this process.

To date, the in vivo efficacy of pepducins has been limited to treating diseases, in which the target cell type is readily accessible. For example, PAR1- and PAR4-targeted pepducin antagonists were demonstrated to have significant efficacy in interdicting platelet thrombosis in mouse and nonhuman primate disease models (Covic et al., 2002; Zhang et al., 2012). In nude mice, P1pal-7 effectively inhibited epithelial-derived lung tumor formation comparably to the current therapeutic standard bevacizumab (Cisowski et al., 2011). A CXCR2 pepducin antagonist inhibited inflammation and spontaneous tumor development by inhibition of CXCR2-rich leukocyte association in an invasive intestinal adenocarcinoma murine model (Jamieson et al., 2012). It should be noted that each of the targeted cell types, such as platelets and

leukocytes, were primarily accessible to circulating pepducins. In a tissue, the target cell types will likely need to have a surface accessible to the bloodstream in order for pepducin delivery. As pepducins do not have a particular targeting mechanism, the hydrophobic N-terminal palmitoyl group will likely incorporate into any membrane that it comes in contact with. In multilayered tissue, the outermost cell type, i.e., epithelial cells in the case of the airway, may act as a sink to capture much of the available pepducin. This hypothesis is corroborated by the phenomena observed while monitoring ASM signaling pathways and contraction in the cell mono-layer in comparison with airway contraction in an ex vivo, intact airway using precision cut lung slices. P4pal-10 was unable to modulate airway contraction in the airway tissue, but exhibited strong efficacy in inhibiting single cell contrac-tion using isolated ASM cells. Additionally, P4pal-10 could inhibit G$_q$-dependent signaling in cell suspension or the monolayer. Plausibly, as the ASM is situated under an epithelial layer, P4pal-10 cannot adequately penetrate the tissue to reach the ASM. In contrast, FR900359 significantly inhibited agonist-promoted contraction in the precision cut lung slices. These observations are likely a commentary on the current therapeutic limitations of the use of pepducins to treat human disease. As previously demonstrated, pepducins can offer novel therapeutic approaches if the targeted cell type is not part of multilayered tissue (i.e., platelets and leukocytes) or it is able to interact with bioavailable pepducin (i.e., lung epithelial tissue). Beyond therapeutic application, it is becom-ing increasingly clear that pepducins, including P4pal-10, can provide unique pharmacological tools and profiles that are not currently ascertainable using orthosteric ligands.

Acknowledgments

Author Contributions

Participated in research design: Carr III, Koziol-White, Lam, An, Panettieri, Benovic.

Conducted experiments: Carr III, Koziol-White, Lam, Zhang.

Contributed new reagents or analytic tools: Carr III, Koziol-White, Panettieri, Tall, An.

Performed data analysis: Carr III, Koziol-White, Panettieri, Benovic.

Wrote or contributed to the writing of the manuscript: Carr III, Koziol-White, An, Panettieri, Tall, Benovic.

References

Al-Muhsen S, Johnson JR, and Hamid Q (2011) Remodeling in asthma. *J Allergy Clin Immunol* **128**:451–462.

An SS, Fabry B, Trepat X, Wang N, and Fredberg JJ (2006) Do biophysical properties of the airway smooth muscle in culture predict airway hyperresponsiveness? *Am J Respir Cell Mol Biol* **35**:55–64.

Bel EH (2013) Clinical practice. Mild asthma. *N Engl J Med* **369**:549–557.

Bernard R, Thach L, Kamato D, Osman N, and Little PJ (2014) Assessing the role of Gαq/11 in cellular responses: an analysis of investigative tools. *Clin Exp Pharmacol* **4**:164.

Billington CK, Kong KC, Bhattacharyya R, Wedegaertner PB, Panettieri RA, Jr, Chan TO, and Penn RB (2005) Cooperative regulation of p70S6 kinase by receptor tyrosine kinases and G protein-coupled receptors augments airway smooth muscle growth. *Biochemistry* **44**:14595–14605.

Bokoch GM, Katada T, Northup JK, Ui M, and Gilman AG (1984) Purification and properties of the inhibitory guanine nucleotide-binding regulatory component of adenylate cyclase. *J Biol Chem* **259**:3560–3567.

Borchers MT, Biechele T, Justice JP, Ansay T, Cormier S, Mancino V, Wilkie TM, Simon MI, Lee NA, and Lee JJ (2003) Methacholine-induced airway hyper-responsiveness is dependent on Galphaq signaling. *Am J Physiol Lung Cell Mol Physiol* **285**:L114–L120.

Canning BJ and Fischer A (2001) Neural regulation of airway smooth muscle tone. *Respir Physiol* **125**:113–127.

Carr R, 3rd, Du Y, Quoyer J, Panettieri RA, Jr, Janz JM, Bouvier M, Kobilka BK, and Benovic JL (2014) Development and characterization of pepducins as Gs-biased allosteric agonists. *J Biol Chem* **289**:35668–35684.

Chan P, Gabay M, Wright FA, Kan W, Oner SS, Lanier SM, Smrcka AV, Blumer JB, and Tall GG (2011a) Purification of heterotrimeric G protein alpha subunits by GST-Ric-8 association: primary characterization of purified G alpha(olf). *J Biol Chem* **286**:2625–2635.

Chan P, Gabay M, Wright FA, and Tall GG (2011b) Ric-8B is a GTP-dependent G protein alphas guanine nucleotide exchange factor. *J Biol Chem* **286**: 19932–19942.

Cisowski J, O'Callaghan K, Kuliopulos A, Yang J, Nguyen N, Deng Q, Yang E, Fogel M, Tressel S, and Foley C et al. (2011) Targeting protease-activated receptor-1 with cell-penetrating pepducins in lung cancer. *Am J Pathol* **179**:513–523.

Cooper PR and Panettieri RA, Jr (2008) Steroids completely reverse albuterol-induced beta(2)-adrenergic receptor tolerance in human small airways. *J Allergy Clin Immunol* **122**:734–740.

Cooper PR, Zhang J, Damera G, Hoshi T, Zopf DA, and Panettieri RA, Jr (2011) C-027 inhibits IgE-mediated passive sensitization bronchoconstriction and acts as a histamine and serotonin antagonist in human airways. *Allergy Asthma Proc* **32**:359–365.

Covic L, Misra M, Badar J, Singh C, and Kuliopulos A (2002) Pepducin-based in-tervention of thrombin-receptor signaling and systemic platelet activation. *Nat Med* **8**:1161–1165.

Deshpande DA and Penn RB (2006) Targeting G protein-coupled receptor signaling in asthma. *Cell Signal* **18**:2105–2120.

Deshpande DA, Wang WC, McIlmoyle EL, Robinett KS, Schillinger RM, An SS, Sham JS, and Liggett SB (2010) Bitter taste receptors on airway smooth muscle bronchodilate by localized calcium signaling and reverse obstruction. *Nat Med* **16**: 1299–1304.

Ediger TL and Toews ML (2000) Synergistic stimulation of airway smooth muscle cell mitogenesis. *J Pharmacol Exp Ther* **294**:1076–1082.

Fabry B, Maksym GN, Butler JP, Glogauer M, Navajas D, and Fredberg JJ (2001) Scaling the microrheology of living cells. *Phys Rev Lett* **87**:148102.

Fujii T and Kawashima K (2000) Ca2+ oscillation and c-fos gene expression induced via muscarinic acetylcholine receptor in human T- and B-cell lines. *Naunyn Schmiedebergs Arch Pharmacol* **362**:14–21.

Fujii T, Yamada S, Watanabe Y, Misawa H, Tajima S, Fujimoto K, Kasahara T, and Kawashima K (1998) Induction of choline acetyltransferase mRNA in human mononuclear leukocytes stimulated by phytohemagglutinin, a T-cell activator. *J Neuroimmunol* **82**:101–107.

Fujioka M, Koda S, Morimoto Y, and Biemann K (1988) Structure of FR900359, a cyclic depsipeptide from *Ardisia-Crenata Sims*. *J Org Chem* **53**:2820–2825.

Gilchrist A, Vanhauwe JF, Li A, Thomas TO, Voyno-Yasenetskaya T, and Hamm HE (2001) G alpha minigenes expressing C-terminal peptides serve as specific inhibitors of thrombin-mediated endothelial activation. *J Biol Chem* **276**: 25672–25679.

Gosens R, Nelemans SA, Grootte Bromhaar MM, McKay S, Zaagsma J, and Meurs H (2003) Muscarinic M3-receptors mediate cholinergic synergism of mitogenesis in airway smooth muscle. *Am J Respir Cell Mol Biol* **28**:257–262.

Hakonarson H and Grunstein MM (1998) Regulation of second messengers associ-ated with airway smooth muscle contraction and relaxation. *Am J Respir Crit Care Med* **158**:S115–S122.

Inamdar V, Patel A, Manne BK, Dangelmaier C, and Kunapuli SP (2015) Charac-terization of UBO-QIC as a Gαq inhibitor in platelets. *Platelets* **26**:771–778.

Jamieson T, Clarke M, Steele CW, Samuel MS, Neumann J, Jung A, Huels D, Olson MF, Das S, and Nibbs RJ et al. (2012) Inhibition of CXCR2 profoundly sup-presses inflammation-driven and spontaneous tumorigenesis. *J Clin Invest* **122**:3127–3144.

Karpinsky-Semper D, Volmar CH, Brothers SP, and Slepak VZ (2014) Differential effects of the Gβ5-RGS7 complex on muscarinic M3 receptor-induced Ca2+ influx and release. *Mol Pharmacol* **85**:758–768.

Kong KC, Billington CK, Gandhi U, Panettieri RA, Jr, and Penn RB (2006) Co-operative mitogenic signaling by G protein-coupled receptors and growth factors is dependent on G(q/11). *FASEB J* **20**:1558–1560.

Krymskaya VP, Orsini MJ, Eszterhas AJ, Brodbeck KC, Benovic JL, Panettieri RA, Jr, and Penn RB (2000) Mechanisms of proliferation synergy by receptor tyrosine kinase and G protein-coupled receptor activation in human airway smooth muscle. *Am J Respir Cell Mol Biol* **23**:546–554.

Luo J, Busillo JM, and Benovic JL (2008) M3 muscarinic acetylcholine receptor-mediated signaling is regulated by distinct mechanisms. *Mol Pharmacol* **74**: 338–347.

McLaughlin JN, Shen L, Holinstat M, Brooks JD, Dibenedetto E, and Hamm HE (2005) Functional selectivity of G protein signaling by agonist peptides and thrombin for the protease-activated receptor-1. *J Biol Chem* **280**:25048–25059.

Moulton BC and Fryer AD (2011) Muscarinic receptor antagonists, from folklore to pharmacology; finding drugs that actually work in asthma and COPD. *Br J Pharmacol* **163**:44–52.

Nishimura A, Kitano K, Takasaki J, Taniguchi M, Mizuno N, Tago K, Hakoshima T, and Itoh H (2010) Structural basis for the specific inhibition of heterotrimeric Gq protein by a small molecule. *Proc Natl Acad Sci USA* **107**:13666–13671.

O'Callaghan K, Kuliopulos A, and Covic L (2012) Turning receptors on and off with intracellular pepducins: new insights into G-protein-coupled receptor drug devel-opment. *J Biol Chem* **287**:12787–12796.

Panettieri RA, Murray RK, DePalo LR, Yadvish PA, and Kotlikoff MI (1989) A hu-man airway smooth muscle cell line that retains physiological responsiveness. *Am J Physiol* **256**:C329–C335.

Pelaia G, Renda T, Gallelli L, Vatrella A, Busceti MT, Agati S, Caputi M, Cazzola M, Maselli R, and Marsico SA (2008) Molecular mechanisms underlying airway

smooth muscle contraction and proliferation: implications for asthma. *Respir Med* **102**:1173–1181.

Scadding GW and Scadding GK (2010) Recent advances in antileukotriene therapy. *Curr Opin Allergy Clin Immunol* **10**:370–376.

Stampfuss JJ, Schrör K, and Weber AA (2003) Inhibition of platelet thromboxane receptor function by a thrombin receptor-targeted pepducin. *Nat Med* **9**: 1447.

Takasaki J, Saito T, Taniguchi M, Kawasaki T, Moritani Y, Hayashi K, and Kobori M (2004) A novel Galphaq/11-selective inhibitor. *J Biol Chem* **279**: 47438–47445.

Taniguchi M, Nagai K, Arao N, Kawasaki T, Saito T, Moritani Y, Takasaki J, Hayashi K, Fujita S, and Suzuki K et al. (2003) YM-254890, a novel platelet aggregation inhibitor produced by *Chromobacterium sp. QS3666*. *J Antibiot (Tokyo)* **56**:358–363.

Zaima K, Deguchi J, Matsuno Y, Kaneda T, Hirasawa Y, and Morita H (2013) Vasorelaxant effect of FR900359 from *Ardisia crenata* on rat aortic artery. *J Nat Med* **67**:196–201.

Zhang P, Gruber A, Kasuda S, Kimmelstiel C, O'Callaghan K, Cox DH, Bohm A, Baleja JD, Covic L, and Kuliopulos A (2012) Suppression of arterial thrombosis without affecting hemostatic parameters with a cell-penetrating PAR1 pepducin. *Circulation* **126**:83–91.

Address correspondence to: Dr. Jeffrey L. Benovic, Department of Biochemistry and Molecular Biology, Thomas Jefferson University, 233 S. 10th St., 926 BLSB, Philadelphia, PA 19107. E-mail: jeffrey.benovic@jefferson.edu